Thermo-Mechanical Reversibility in a Shape Memory Organic Salt

Subham Ranjan, Hisashi Honda* and Satoshi Takamizawa*

Department of Materials System Science, Graduate School of Nanobioscience,

Yokohama City University

22-2 Seto, Kanazawa-ku, Yokohama, Kanagawa 236-0027 (Japan)

E-mail: hhonda@yokohama-cu.ac.jp; staka@yokohama-cu.ac.jp

Table of contents: **Page**

Other supporting material

Stress- and thermal-induced deformation behaviors under the microscope:

Movie S1. Thermal-induced mechanical deformation α → β and β→α transformation and shearing-induced mechanical deformation α → β and β→α transformation.

Movie S2. Shearing-induced mechanical deformation α to β at 32 ºC temperature and thermal-induced reverse transformation β → α at 39 ºC temperature.

Movie S3. Stress-displacement test on $(\bar{1}12)$ and $(\bar{1}1\bar{1})$ planes at 32 ºC and 39 ºC, respectively.

Movie S4. Stress-displacement test on $(\bar{1}12)$ plane at 38.9 ºC temperature.

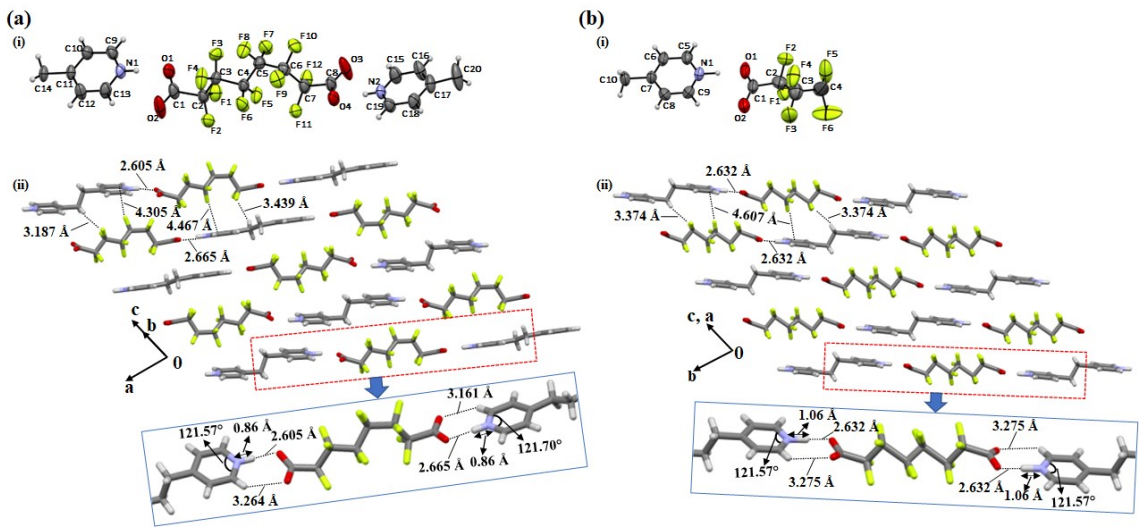

Figure S1. ORTEP view and crystal packing of **(a)** α form and **(b)** β form. (a)(i) and (b)(i) are the ORTEP view of α form and β form with 50% probability of displacement ellipsoids, respectively. Both forms have triclinic system with $P\bar{1}$ space group with Z = 2. (a)(ii) and (b)(ii) are the crystal packing of α form and β form with the analysis of synthons, C—N—C bonds and N—H distances, respectively.

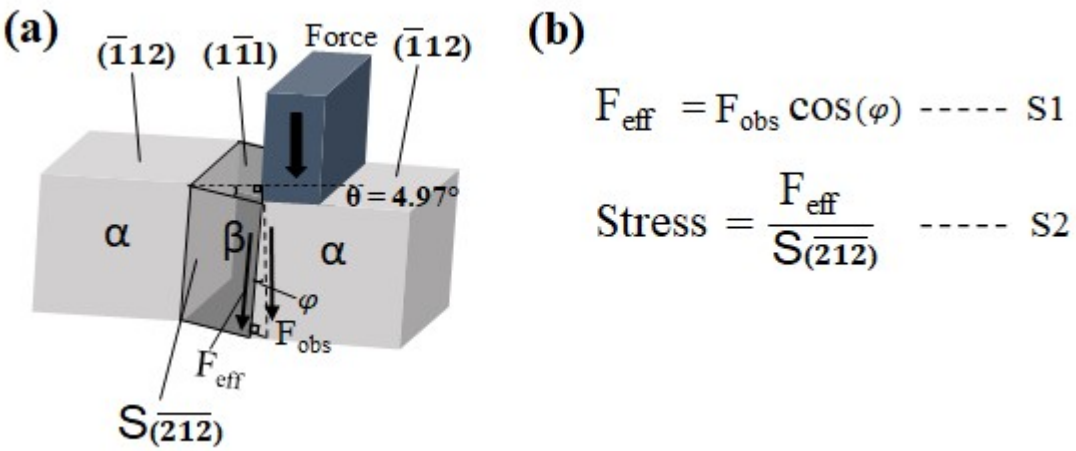

Figure S2. (a) Experimental setup and (b) Calculation of effective stress. Equations S1 and S2 are the calculation of effective force and effective stress, respectively.

Table S1. Comparison of mechanical parameters of organosuperelastic crystals.

Compounds	Mechanism	σ_f / MPa	σ_r / MPa	E_s / kJ m^{-3}	η	χ	θ / °
Terephthalamide[1]	Phase transition	0.50	0.46	62	0.93	0.13	6.5
5-Tetrabutyl-n-phosphonium tetraphenylborate[2]	Phase transition	0.53	0.42	50	0.79	0.10	5.3
7-Chloro-2-(2'-hydroxyphenyl)imidazo[1,2-a]pyridine[3]	Phase transition	1.53	0.66	560	0.43	0.51	42.1
Salt **(32 °C)**	Phase transition	2.27	1.65	18	0.72	0.01	4.97
Salt **(47 °C)**	Phase transition	3.21	3.07	26	0.92	0.01	4.97

Mechanism of superelasticity: mechanical twinning and mechanically-induced phase transition. Effective shear stress for deformation: proceeding in the forward (σ_f) and reverse (σ_r) directions. Energy storage density ($E_s=W_{in}/V$). The symbols W_{out} and V represent the output work and volume, respectively, in a deformed region of the specimen during superelastic deformation. Energy storage efficiency ($\eta=W_{out}/W_{in}$) where W_{in} represents input work. Superelastic index ($\chi=2E/(\sigma_f+\sigma_r)$). θ represents the crystal bending angle.

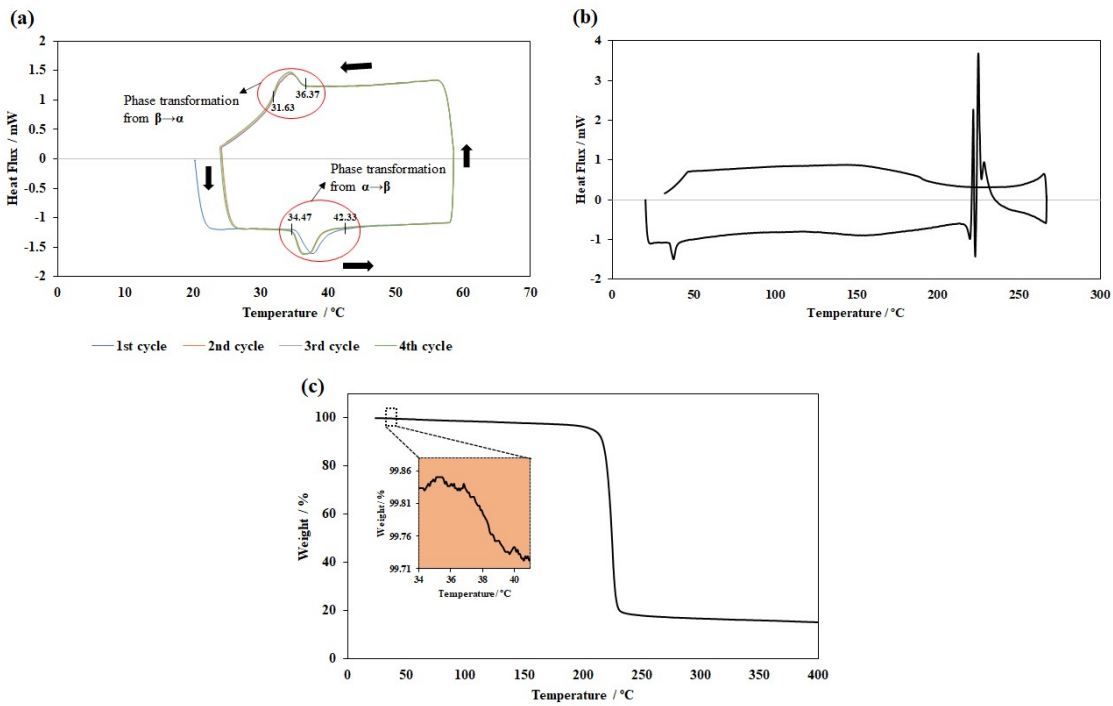

Figure S3. DSC curves of **1** during four consecutive heating-cooling cycles **(a)** and the one over decomposition **(b)**. TG profile of **1** with the magnified region during a staircase weight loss due to α to β transition **(c)**.

Table S2. **Crystallographic data of α and β, and hydrate form of crystal 1.**

Domain	α	β	Hydrate salt
T /K	305(2)	312(2)	123(2)
Empirical formula	$C_{20}H_{14}F_{12}N_2O_4$ (Mother Domain)	$C_{10}H_7F_6NO_2$ (Daughter Domain)	$C_{14}H_{09}F_{12}NO_5$
Crystal system	triclinic	triclinic	triclinic

Space group	$P\bar{1}$	$P\bar{1}$	$P\bar{1}$
a/Å	9.2422(2)	7.1050(3)	9.0200(5)
b/Å	9.2641(2)	8.9389(4)	9.6306(5)
c/Å	13.4983(4)	9.3188(4)	11.2785(6)
α /°	84.1350(10)	84.101(2)	68.659(2)
β /°	74.7540(10)	82.567(2)	73.934(2)
γ /°	85.0570(10)	73.593(2)	88.879(2)
V /Å^3	1107.10(5)	561.61(4)	873.50(8)
Z	2	2	2
ρ_{calcd} [g cm^{-3}]	1.723	1.698	1.898
F(000)	576	288	496
μ [mm^{-1}]	0.185	0.183	0.221
index ranges	-11 ≤ h ≤ 10, -8 ≤ k ≤ 11, -12 ≤ l ≤ 16	-6 ≤ h ≤ 8, -10 ≤ k ≤ 10, -8 ≤ l ≤ 11	-9 ≤ h ≤ 10, -11 ≤ k ≤ 8, -13 ≤ l ≤ 13
Reflections collected	7282	3640	6170
Goodness of fit	1.023	1.048	1.108
R_1(*I*> 2σ (all	0.0654	0.0919	0.0346

data))			
wR_2(I> 2σ (all data))	0.2068	0.2985	0.1115
CCDC No.	2168787	2168788	2168789

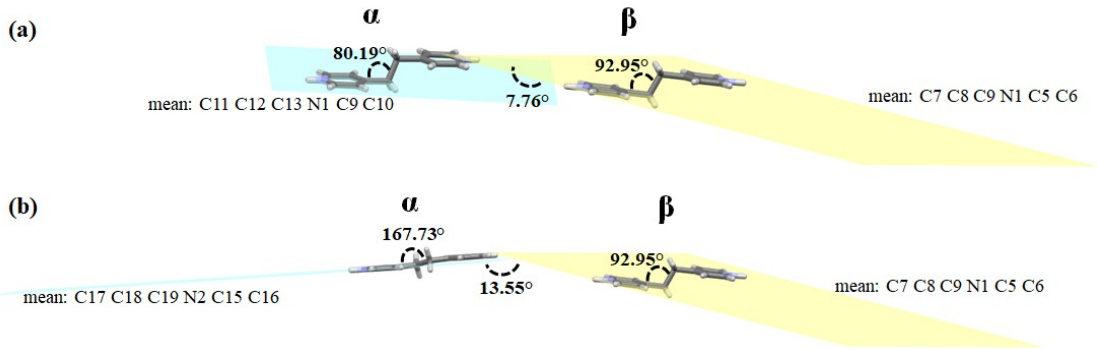

Figure S4. Torsional and dihedral angles on and between bipyridines: **(a)** bipyridine (A) moiety of α form was compared with bipyridine (A) moiety of β form, and **(b)** bipyridine (A') moiety of α form was compared with bipyridine (A) moiety of β form.

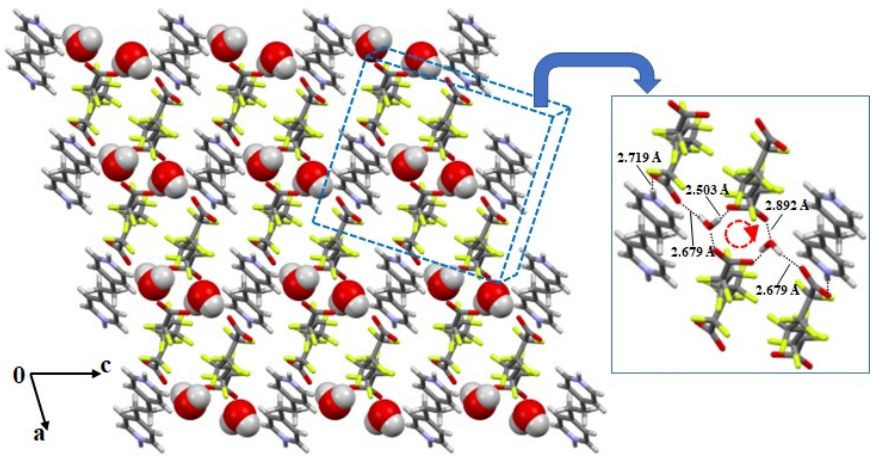

S⊠

Figure S5. Crystal packing of salt hydrate along the b-axis (water molecules with a space fill model). The inset highlights the 10-membered ring ($R_4^4(10)$ in the hydrogen bonding network with a capped sticks model.

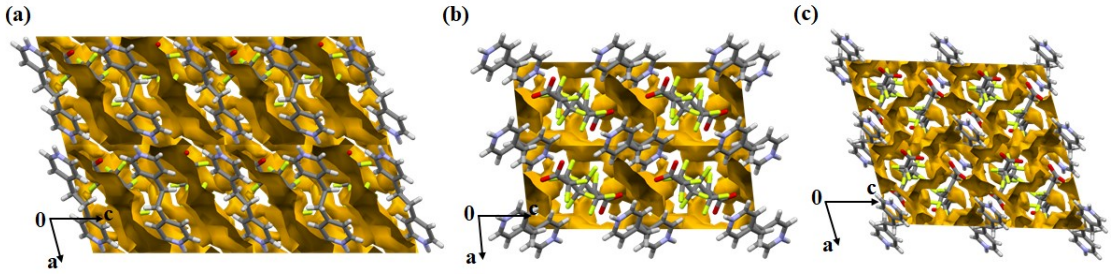

Figure S6. Void surfaces **(a)** α form, **(b)** β form, and **(c)** hydrate form.

Table S3: Void volume of unit cell volume and % empty space in α and β, and hydrate forms.

S.No.	Volume (Å^3)	% Empty space of unit cell vol.
α form	175.10	15.8
β form	79.67	14.2
Hydrated form	110.11	12.6

Three-Point Bending Tests. Variable temperature three-point bending test experiments were conducted by using a universal testing machine coupled with a thermal controlled stage. A single crystal was put on two-point support and a metal-blade jig was used to apply stress to the crystal (Fig. S5). At a displacement rate of 3 m sec^{-1}, the jig pushed the crystal face ($01\bar{2}/0\bar{1}2$ in α form and $\bar{1}01/10\bar{1}$ in β form) downward (press). The tension was released after bending, and the deformation behavior was observed using a polarized

microscope. The displacement with respect to the applied force is calculated using the three-point bending test. The following equation, where L is the support span (mm) and D is the deflection of the center, is then used to convert it to stress and strain (mm).

$$\text{Stress} = \frac{3\times\text{Force}\times L}{2\times\text{width}\times\text{height}^2} \quad \cdots\cdots\cdots\cdots \quad \text{S1}$$

$$\text{Strain} = \frac{6\times D\times\text{height}}{L^2} \quad \cdots\cdots\cdots\cdots \quad \text{S2}$$

$$\text{Elastic Modulus} = \frac{\text{Stress}}{\text{Strain}}$$

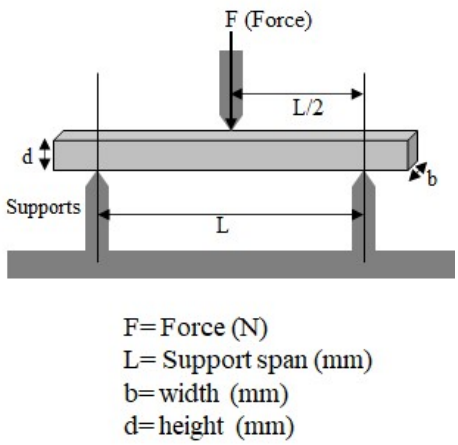

Figure S7. Experimental setup. A single-crystal specimen was supported on two points, and a metal-blade jig was used to apply the load to the crystal.

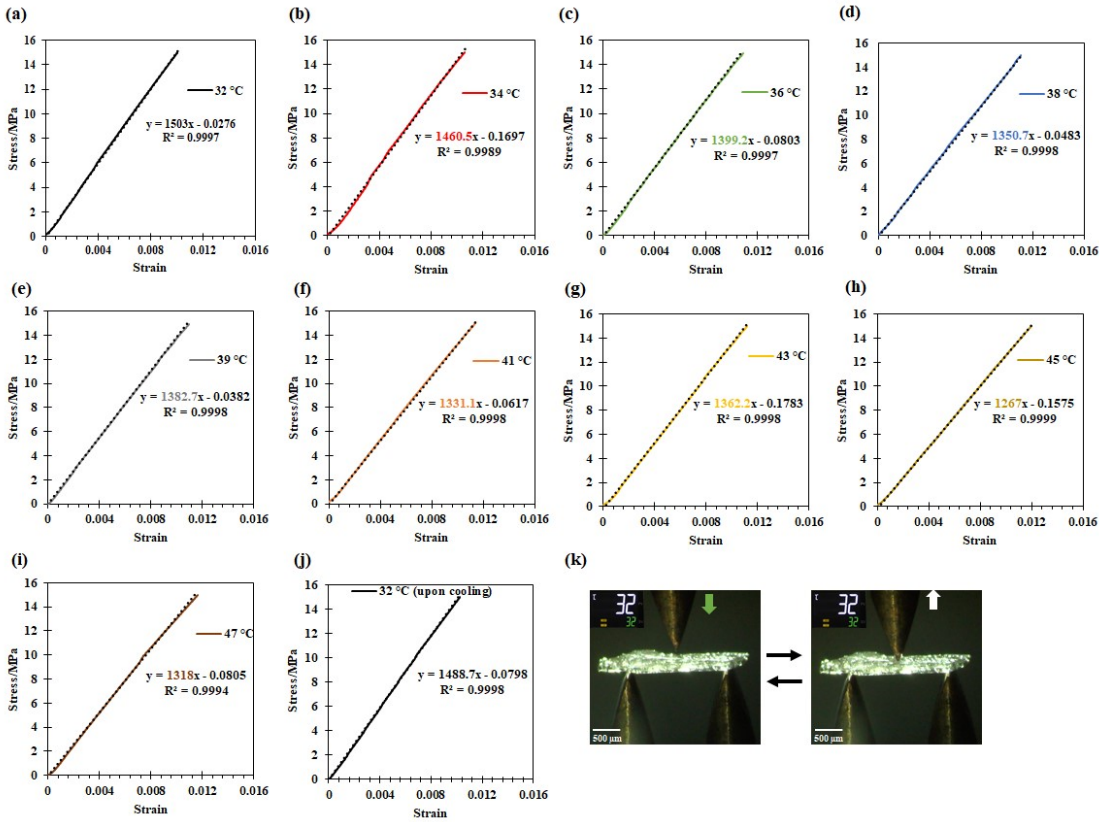

Figure S8. Stress-Strain curves of crystal **1** recorded by three-points bending at 32 to 47 ºC with the slope gradient giving elastic modulus.

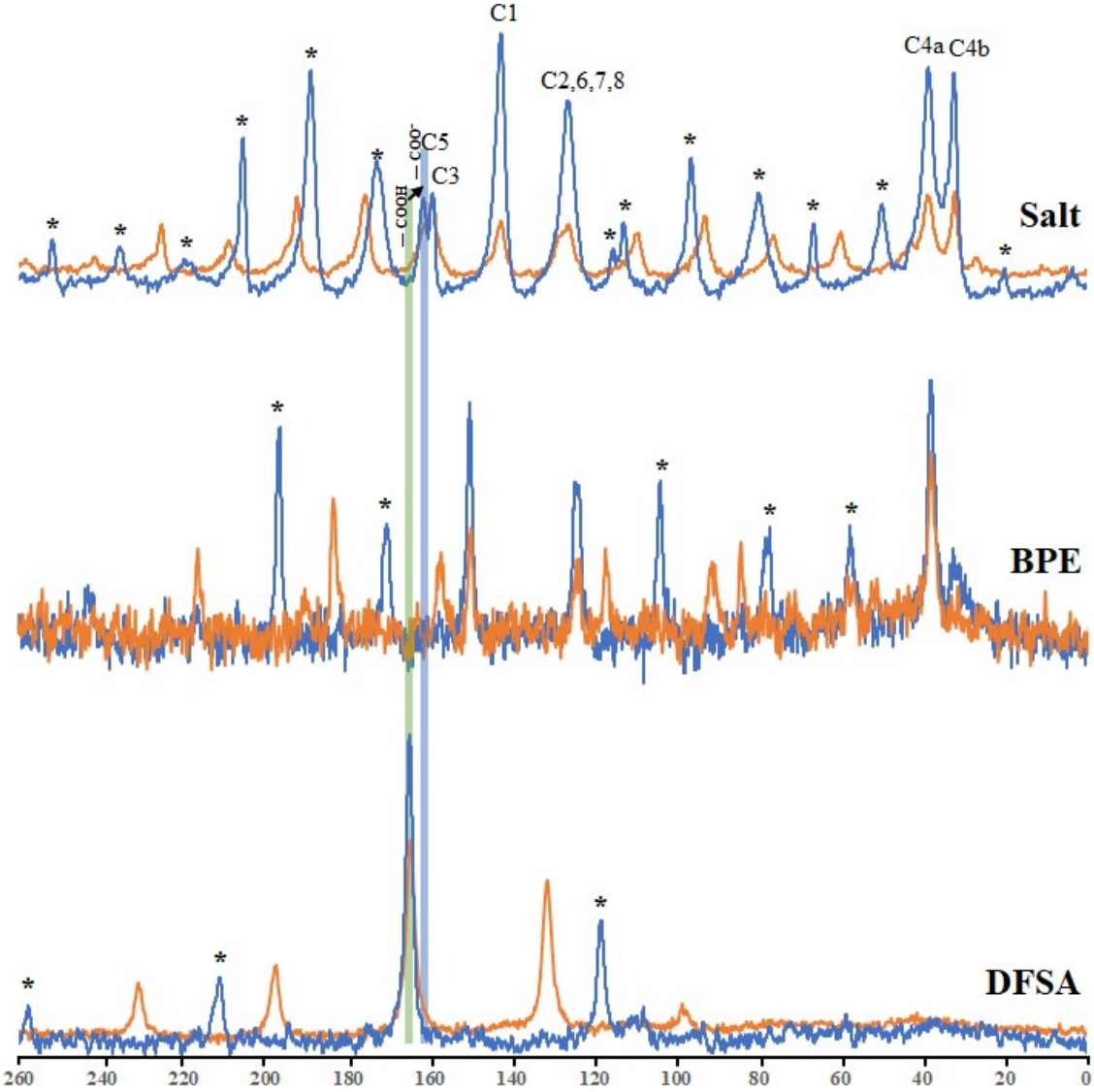

Figure S9. The Solid-state ^{13}C CP/MAS NMR spectrum of crystal **1,** 1,2-bis (4-pyridyl) ethane (BPE) and dodecafluorosuberic acid (DFSA) measured at 5 kHz (orange) and 7 kHz (blue) at room temperature. Asterisks denote the spinning sidebands. The up-field shift from 164.6 ppm to 161.8 ppm in the carbonyl carbon of the DFSA is colored in light green and blue, respectively.

(a)

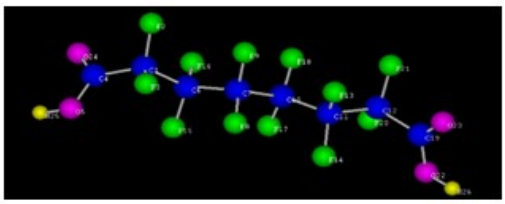

Routet: B3LYP/6-311+G**
Comments: acid_nmr
Charge = 0 Multiplicity = 1
Number of Atoms: 26

Chemical Shift: Shielding Tensor of TMS 1H 13C 184.0118

Number	Atom	Shielding Tensor (Iso)	Chemical Shift (ppm)	Anisotopy (ppm)	XX Component	YY Component	ZZ Component
1	C	65.2907	118.7211	16.1917	136.6316	111.605	107.9266
2	F	283.5509	283.5509	95.8883	190.8819	312.2943	347.4764
3	F	298.3601	298.3601	84.4156	205.0134	335.4296	354.6371
4	C	17.8754	166.1364	83.49	271.9089	116.0239	110.4764
5	O	118.5912	118.5912	177.7754	-47.2876	165.953	237.1081
6	C	63.3863	120.6255	14.2046	135.9219	114.7988	111.1557
7	C	62.7194	121.2924	14.7345	135.7211	116.6868	111.4694
8	F	293.2976	293.2976	81.1953	211.4745	320.9905	347.4278
9	F	293.3501	293.3501	83.5257	211.3182	319.6981	349.0338
10	C	62.7193	121.2925	14.7344	135.7211	116.6869	111.4696
11	C	63.3869	120.6249	14.2047	135.9218	114.7978	111.1551
12	C	65.2908	118.721	16.1933	136.6326	111.6049	107.9254
13	F	297.352	297.352	83.4278	211.4441	327.6414	352.9706
14	F	289.2307	289.2307	75.4833	206.7489	321.3903	339.5529
15	F	289.229	289.229	75.4786	206.7457	321.3931	339.548
16	F	297.3533	297.3533	83.4331	211.45	327.6346	352.9754
17	F	293.2965	293.2965	81.1944	211.4724	320.9911	347.4261
18	F	293.3506	293.3506	83.5272	211.3203	319.696	349.0354
19	C	17.8768	166.135	83.4886	271.9072	116.0219	110.4759
20	F	298.3589	298.3589	84.4233	205.0035	335.4321	354.6411
21	F	283.5592	283.5592	95.8856	190.8938	312.3008	347.4829
22	O	118.5915	118.5915	177.777	-47.2878	165.9528	237.1095
23	O	-110.871	-110.871	577.8765	-347.709	-259.284	274.3797
24	O	-110.866	-110.866	577.8686	-347.697	-259.281	274.3794
25	H	25.572	6.411549	12.5471	11.80335	9.38435	-1.95325
26	H	25.572	6.411549	12.5471	11.80345	9.38435	-1.95325

(b)

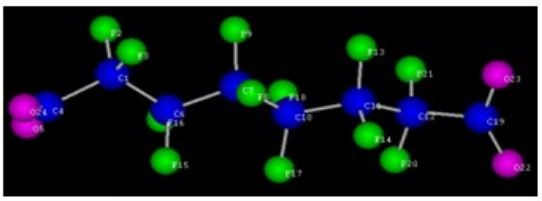

Routet: B3LYP/6-311+G**
Comments: acid anion_nmr
Charge = -2 Multiplicity = 1
Number of Atoms: 24

Chemical Shift: Shielding Tensor of TMS 1H 13C 184.0118

Number	Atom	Shielding Tensor (Iso)	Chemical Shift (ppm)	Anisotopy (ppm)	XX Component	YY Component	ZZ Component
1	C	62.4932	121.5186	18.4531	138.8001	116.5392	109.2165
2	F	285.9019	285.9019	112.1914	175.4649	321.5446	360.6961
3	F	288.4325	288.4325	79.3517	200.1022	323.8616	341.3336
4	C	20.3923	163.6193	107.7841	265.7701	133.3247	91.7632
5	O	6.1859	6.1859	333.1269	-183.178	-26.535	228.2705
6	C	60.7843	123.2275	16.6845	137.3642	120.2138	112.1046
7	C	60.3622	123.6496	14.8835	136.476	120.7454	113.7272
8	F	293.6888	293.6888	79.7146	210.7338	323.5008	346.8319
9	F	294.8934	294.8934	81.675	210.4334	324.9035	349.3435
10	C	60.363	123.6488	14.8872	136.476	120.7464	113.724
11	C	60.7883	123.2235	16.6741	137.3599	120.2032	112.1075
12	C	62.4856	121.5262	18.4608	138.8252	116.5344	109.219
13	F	294.6066	294.6066	76.804	211.2752	326.7354	345.8093
14	F	292.3843	292.3843	73.3627	206.6373	329.2228	341.2928
15	F	292.3722	292.3722	73.3597	206.6105	329.2274	341.2787
16	F	294.6063	294.6063	76.821	211.3049	326.6938	345.8204
17	F	293.6931	293.6931	79.7143	210.7388	323.5045	346.8359
18	F	294.9002	294.9002	81.6844	210.4461	324.8981	349.3565
19	C	20.3948	163.617	107.7953	265.7675	133.33	91.7534
20	F	288.4534	288.4534	79.4748	200.0512	323.8723	341.4366
21	F	285.9041	285.9041	112.2144	175.4646	321.5341	360.7137
22	O	-0.1535	-0.1535	345.5856	-196.84	-33.8573	230.2369
23	O	6.1634	6.1634	333.1856	-183.27	-26.5269	228.2871
24	O	-0.1472	-0.1472	345.5359	-196.802	-33.8497	230.2101

Figure S10. A B3LYP/6311+G** function was used to estimate the ^{13}C NMR peaks of dodecafluorosuberic acid in (a) neutral and (b) anion form. The highlighted values indicate the up-field shift in the carbonyl carbon peak of the dodecafluorosuberic acid which was also seen in α form of crystal **1**.

(a)

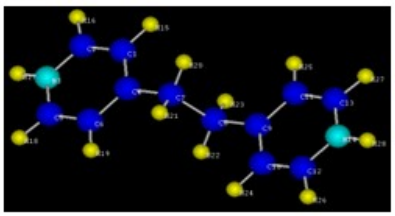

Routet: #p B3LYP/6-311+G** nmr
Comments: Chair bipyridine cation NMR
Charge = 2 Multiplicity = 1
Number of Atoms: 28

Chemical Shift	Shielding Tensor of TMS	1H		13C	184.0118		
Number	Atom	Shielding Tensor (Iso)	Chemical Shift (ppm)	Anisotopy (ppm)	XX Component	YY Component	ZZ Component
	1C	47.6256	136.3862	178.7626	241.0309	150.9165	17.21109
	2C	35.2612	148.7506	179.0992	247.3168	169.5839	29.3512
	3N	51.7077	51.7077	251.6783	-101.417	37.0467	219.4932
	4C	9.9551	174.0567	243.4969	274.8957	235.549	11.72549
	5C	34.868	149.1438	179.5693	247.8762	170.1243	29.43089
	6C	47.3664	136.6454	179.0254	241.4403	151.2006	17.29509
	7C	139.5784	**44.4334**	38.355	59.52499	54.91179	18.86339
	8C	139.5698	**44.442**	38.3557	59.56979	54.8848	18.8716
	9C	10.0039	174.0079	243.4959	274.7045	235.642	11.67729
	10C	47.696	136.3158	178.7384	240.8909	150.8996	17.15689
	11C	47.5231	136.4887	178.9158	241.24	151.0146	17.2115
	12C	34.966	149.0458	179.4296	247.6366	170.0747	29.4261
	13C	34.6406	149.3712	179.1588	248.1625	170.0191	29.93199
	14N	51.2329	51.2329	252.1975	-102.014	36.3483	219.3646
	15H	23.6414	8.34215	8.0621	12.11375	9.94525	2.967449
	16H	23.1336	8.849949	5.0861	13.17635	7.914249	5.459148
	17H	21.4835	10.50005	5.8132	16.79105	8.084549	6.62455
	18H	23.1269	8.856649	5.1	13.17445	7.938848	5.45665
	19H	23.6231	8.360449	8.0578	12.10775	9.984949	2.988548
	20H	28.676	3.307549	4.8956	7.423248	2.455549	0.04385
	21H	28.6733	3.310249	4.8975	7.432348	2.453049	0.04525
	22H	28.672	3.311548	4.8946	7.43215	2.453949	0.048449
	23H	28.6742	3.309349	4.8947	7.426748	2.45505	0.046148
	24H	23.6434	8.340149	8.0507	12.10975	9.93775	2.973049
	25H	23.6353	8.348249	8.0526	12.11245	9.952549	2.97995
	26H	23.1202	8.86335	5.0907	13.18265	7.937948	5.469549
	27H	23.1099	8.87365	5.1023	13.16615	7.982649	5.47205
	28H	21.4878	10.49575	5.773	16.75935	8.08075	6.647049

(b)

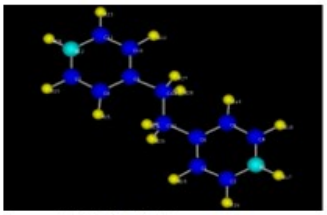

Routet: #p B3LYP/6-311+G** nmr
Comments: Planar bipyridine cation mm2_nmr
Charge = 2 Multiplicity = 1
Number of Atoms: 28

Chemical Shift	Shielding Tensor of TMS	1H		13C	184.0118		
Number	Atom	Shielding Tensor (Iso)	Chemical Shift (ppm)	Anisotopy (ppm)	XX Component	YY Component	ZZ Component
	1C	55.4342	128.5776	167.8092	229.6351	139.3929	16.70479
	2C	45.1507	138.8611	173.3525	229.1488	164.1416	23.29269
	3N	65.183	65.183	234.2293	-80.8751	55.0883	221.3359
	4C	43.7183	140.2935	174.6911	231.1592	165.8885	23.8327
	5C	60.8906	123.1212	172.7193	225.5323	135.8563	7.975098
	6C	23.4455	160.5663	233.5914	259.9722	216.8879	4.838699
	7C	43.7146	140.2972	174.7288	231.2242	165.8561	23.8114
	8C	60.8914	123.1204	172.6583	225.5816	135.7647	8.014801
	9C	23.485	160.5268	233.5745	259.9001	216.8699	4.810501
	10C	55.497	128.5148	167.7552	229.5531	139.3132	16.67799
	11C	45.177	138.8348	173.3687	229.2059	164.0428	23.2556
	12N	65.2507	65.2507	234.0756	-80.665	55.1161	221.3011
	13C	147.2791	**36.7327**	25.6878	51.2802	39.31039	19.6075
	14C	147.1779	**36.83389**	25.727	51.5486	39.2706	19.6826
	15H	23.6633	8.32025	8.1928	13.01485	9.08745	2.85845
	16H	23.4151	8.568449	4.6082	13.81065	6.39835	5.496349
	17H	21.0191	10.96445	6.7985	17.34515	9.116049	6.43215
	18H	23.392	8.591549	5.2199	13.95475	6.708149	5.111549
	19H	23.8854	8.098148	9.5829	13.65165	8.933249	1.709549
	20H	23.3919	8.59165	5.2154	13.95155	6.70875	5.11475
	21H	23.8851	8.09845	9.564	13.63925	8.933649	1.722448
	22H	23.6646	8.318949	8.1935	13.01215	9.08815	2.856548
	23H	23.4154	8.56815	4.6067	13.80645	6.401049	5.497049
	24H	21.0237	10.95985	6.811	17.34945	9.110949	6.419149
	25H	27.8525	4.131048	6.353	9.886549	2.610849	-0.10425
	26H	27.8396	4.14395	6.3424	9.91095	2.605249	-0.08425
	27H	27.84	4.143549	6.3119	9.903749	2.591249	-0.06445
	28H	27.85	4.133549	6.3415	9.915949	2.578749	-0.09415

Figure S11. A B3LYP/6311+G** function was used to estimate the ^{13}C NMR peaks of 1,2-bis(4-pyridyl) ethane in (a) chair and (b) planar form. The highlighted values indicate the conformational changes which were seen in the α form of crystal **1**.

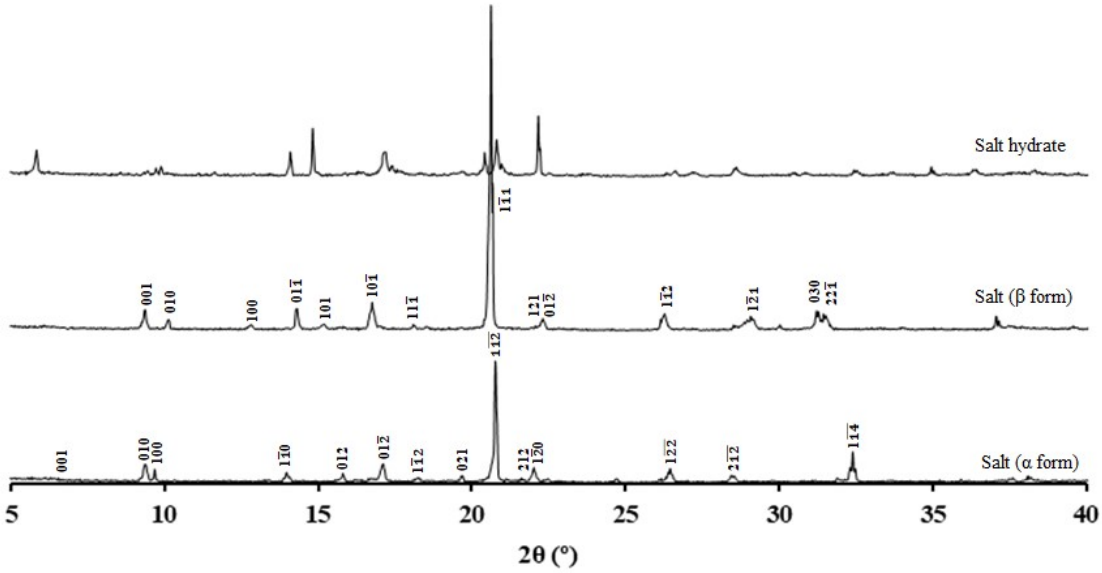

Figure S12. Powder X-ray diffraction patterns of the α, β, hydrated forms of crystal **1**.

References

1. S. Takamizawa and Y. Miyamoto, *Angew. Chem.*, 2014, **126**, 7090-7093.

2. S. Takamizawa and Y. Takasaki, *Chem. Sci.*, 2016, **7**, 1527-1534.

3. T. Mutai, T. Sasaki, S. Sakamoto, I. Yoshikawa, H. Houjou, S. Takamizawa, *Nat. Commun.,* 2020, ***11***, 1-6.